APPLICATION OF MAGENTIC MICRO-FLUID CHIP TO CHEMICAL AND ELECTROCHEMICAL REACTIONS

R. Aogaki, E. Ito, M. Ogata

Dept. of Product Design, Polytechnic University 4-1-1, Hashimoto-dai, Sagamihara, 229-1196, Japan (aogaki@uitec.ac.jp)

Introduction. In a magnetic field, chemical and electrochemical reactions generate some kinds of forces; one is the Lorentz force, and others are magnetic forces. The Lorentz force is induced by the interaction between an electrolytic current and a magnetic field, so that the electrolyte solution starts to move, and MHD (magnetohydrodynamic) flow and micro-MHD flows emerge. These flows sometimes enhance the mass transfer process of active species (MHD effect) [1]–[6], and sometimes suppress the autocatalytic reactions such as electrodeposition and metal corrosion (micro-MHD effect) [7]–[11]. On the other hand, magnetic forces are generated by heterogeneous and homogeneous magnetic fields, which are obtained by differentiating the magnetic energy stored in a unit volume with respect to position. The homogeneous force is generated in a homogeneous magnetic field [12]–[14], whereas in a heterogeneous magnetic field a heterogeneous magnetic force is induced [15, 16]. The former becomes weaker than the latter. However, the latter, the heterogeneous magnetic force, becomes of the same level as the Lorentz force. Characteristic magneto-convection in a heterogeneous magnetic field has been theoretically and experimentally established [17]–[20]; especially, in a magnetic field vertical to the crystal surface of copper sulfate with paramagnetism, it was clarified that numerous minute convection cells with approximately $10\,\mu$ m in size emerge in front of the dissolved surface [19, 20]. Recently, in a magnetic field vertical to a micro-electrode surface, the same type of convection was measured by the increase of diffusion current [21].

Micro-fluid chips are now developing with other technologies such as DNA sequencing, which are composed of a network of solid channels fabricated inside a glass or plastic plate [22]. As a result, several problems inevitably arise; for the improvement of the efficiency of the processing, cross-sectional areas of each channel should be decreased, so that the channels are easily choked up with small particles or bubbles contaminated in test solutions. Moreover, as the cross-section decreases, the pressure difference for driving liquids becomes higher, and resultantly, it becomes more difficult to smoothly operate the multi-channel fluid chips.

In this paper, therefore, as an attempt for removing the obstacles completely, instead of solid channels, magnetic channels surrounded by magnetic walls (i.e., magnetic barriers) are proposed. The magnetic walls can confine fluids to the magnetic channels by the heterogeneous magnetic force. These channels do not have any solid walls, so that a test solution inside the channel smoothly proceeds as if a completely non-viscous fluid. Moreover, since the magnetic channel is surrounded by not a solid material, but by other fluid called an environmental solution, the heat or mass transfer through the magnetic wall is possible. Such situation is also useful for chemical and electrochemical reactions through the magnetic wall. As the first step to establish the proposed magnetic micro-fluid chip, the non-viscous nature of the magnetic-channel fluid is clarified, and then some applications are examined.

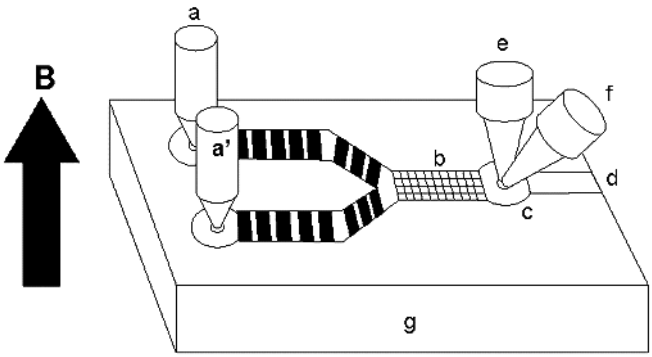

Fig. 1. Concept of the magnetic micro-fluid chip a – inlet of test solution; a' – inlet of reagent solution; b – mixing chamber; c – detection area; d – outlet; e – laser; f – detector; g – chip plate; B – magnetic flux density.

1. Theoretical. Fig. 1 shows the basic concept of a magnetic micro-fluid chip [23]; the test and reagent solutions are introduced to the chip from two inlets to two magnetic channels. The solutions move along two metal tracks imbedded on a chip surface, where the magnetic channels are formed on the tracks. Then, the solutions are reacted at a mixing chamber, which is also made of the magnetic walls. Finally, at the end of the channel, with a proper monitoring system (e.g., a laser detection system), the reaction product is detected. Fig. 2a exhibits the schematic figure of the magnetic walls (i.e., magnetic barriers) formed around a track made of ferromagnetic materials. As shown in Figs. 2b and 2c, under a magnetic field, in the neighborhood of ferromagnetic materials, or sometimes diamagnetic materials, the magnetic flux density has a heterogeneous distribution; inside a ferromagnetic material, the magnetic flux density increases than the outside, whereas the magnetic flux density decreases inside a diamagnetic material; the magnetic flux density outside the ferromagnetic material decreases, and outside the diamagnetic materials, the magnetic flux density increases. As a result, a heterogeneous distribution of magnetic flux density, i.e., a magnetic barrier (mag-

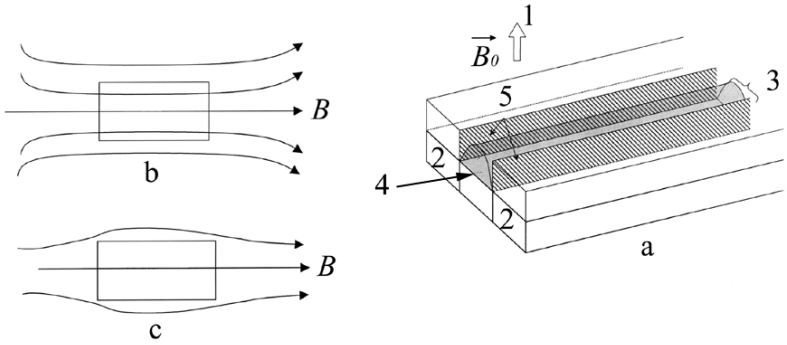

Fig. 2. Formation of a magnetic channel. (a) Schematics of magnetic walls for a diamagnetic solution. 1 – magnetic flux density; 2 – ferromagnetic material; 3 – diamagnetic material; 4 – diamagnetic solution; 5 – magnetic wall. (b) Distribution of the magnetic flux density around a ferromagnetic material. (c) Distribution of the magnetic flux density around a diamagnetic material.

netic wall) is formed. Generally, the magnetic force acting on a material in a heterogeneous magnetic field can be expressed by

$$\mathbf{f} = -\frac{\Delta\chi}{\mu_0}\mathbf{B}\nabla\mathbf{B} \tag{1}$$

where μ_0 is the magnetic permeability, $\mathbf{B}$ is the magnetic flux density, and $\nabla\mathbf{B}$ is the gradient of $\mathbf{B}$. $\Delta\chi$ is a relative dimensionless magnetic susceptibility, where $\Delta\chi \equiv \chi_t - \chi_e$ is defined, and χ_t and χ_e are the dimensionless susceptibilities of the test solution and the surrounding solution called "environmental solution", respectively. According to the relative susceptibility and the distribution of the magnetic flux density, around a track on a chip surface, the test solution is trapped inside the magnetic barrier. The same type of magnetic barrier can be produced not only along the chip surface, but also vertical to the surface, so that a magnetic channel surrounded by the magnetic walls is completed. Moreover, a vertical distribution of the magnetic flux density produces buoyancy for the test solution. As shown in Fig. 3, in the vertical bore space of a superconducting magnet, the magnetic flux density distributes around a maximum magnetic center, so that Eq.(1) is also applicable to the vertical direction. For example, for an apparent paramagnetic solution, on the lower side of the magnetic center, upward (positive) buoyancy is newly added, whereas on the upper side, downward (negative) buoyancy is imposed. As mentioned above, since apparent magnetism of the test solution is determined by the relative susceptibility between the test solution and the environmental solution, if the environmental solution shows strong paramagnetism, a weak diamagnetic test solution can be treated as a strong diamagnetic material. On a track with ferromagnetism shown in Fig. 2, a magnetic channel for a paramagnetic solution is formed, whereas between the two tracks, a magnetic channel for a diamagnetic solution is formed.

2. Experimental. As a test solution, $1.4\,\mathrm{mol\,dm^{-3}}$ nickel sulfate solution ($NiSO_4$, paramagnetic) was used, and as a corresponding environmental solution, pure water (diamagnetic) was adopted. To measure the velocity of the solution, carbon colloid was, as a tracer, added to the test solution. To observe the non-viscous feature of two test solutions in mixing, the same nickel sulfate solutions were colored by black and white watercolors. The black-colored solution was also used for visualizing a magnetic channel in static state. With two test

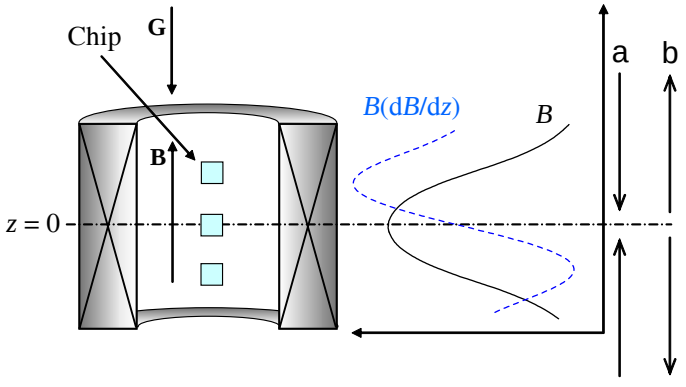

Fig. 3. Distribution of the magnetic flux density in a bore space of a superconducting magnet. (*a*) Direction of the magnetic force imposed to apparent paramagnetic solution; (*b*) Direction of the magnetic force imposed to apparent diamagnetic solution. **B** – magnetic flux density; $(\mathrm{d}B/\mathrm{d}z)$ – vertical gradient of the magnetic flux density; **G** – gravitational acceleration.

solutions of different viscosities, the flow velocities were measured; the viscosities were controlled with adding starch to the solutions, and carbon colloid was also added as a tracer for measuring the velocities. A superconducting magnet (HF10-100VHT, Sumitomo Heavy Industries, Ltd.) was used for generating the magnetic field up to 10 T, of which the bore space with 10 cm diameter was vertically set up. By changing the vertical position of a chip in the bore space, as discussed in Sec. 1. Theoretical, the intensities of the upper- and lower-vertical magnetic barriers were changed; when the upper side of the magnetic center was selected, the barriers for a paramagnetic test solution were reinforced, whereas on the lower side, the barriers were weakened. The metal tracks were made of iron plates (1 mm thick and 1 mm wide) with various lengths. A special track with two bulges (5 mm wide and 10 mm long) was prepared for the mixing chambers. The iron tracks were imbedded onto an epoxy resin plate, and the surface covered with epoxy resin was roughly polished. In comparison, another fluid chip with channels composed of solid walls with the same widths as the metal tracks of the magnetic channels was also prepared; except for the upper parts, the channels were surrounded by plastic solid walls, and used in zero magnetic field. The magnetic micro-fluid chips were immersed into pure water in a glass vessel, which was settled at a given position in the bore space. The test solutions were introduced to the magnetic channels with homemade syringes. At the end of the channels, the solutions were recovered with other syringes.

3. Results and discussion. To visualize the static structure of the magnetic channel, a black test solution was injected into the channel with closed ends until spilling out of the channel. As shown in Fig. 4, the cross-section of the channel took a circular shape, the size of which depended on the strength of the vertical magnetic barriers. This is because the magnetic force balanced with the gravity force mainly determines the static shape. In this figure, the maximum size of the cross-section is exhibited. The magnetic force sustains the test solution forming a round bottom, so that almost all the bottom of the solution floats from the chip surface, i.e., the test solution is surrounded by frictionless liquid interfaces. From this characteristic feature of the magnetic-channel fluid, just like the maglev, quite smooth frictionless motion can be realized.

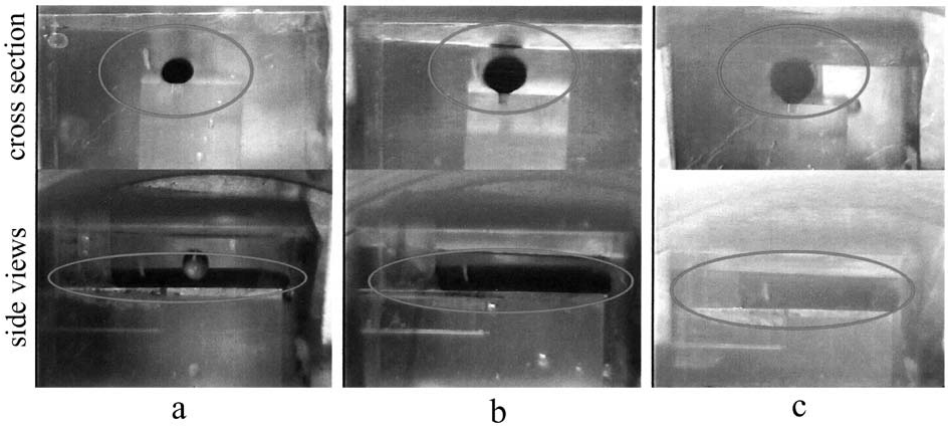

Fig. 4. Visualization of the magnetic channels in static state. (*a*), at 9 cm above the magnetic field center (downward buoyancy is applied); (*b*), at the magnetic field center (buoyancy is not applied); (*c*), at 9 cm below the magnetic center (upward buoyancy is applied).

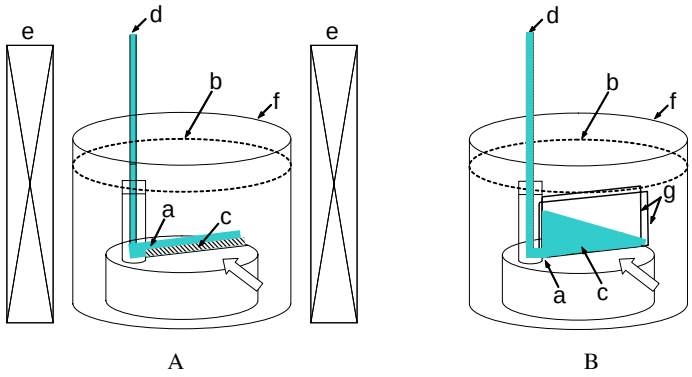

Fig. 5. Experimental setups for observing solution flows. (A) Solution flow in a magnetic channel. a – inlet; b – water; c – iron track; d – test solution; e – magnet; f – vessel. (B) Solution flow in a solid channel made of a solid bottom and two solid walls. a – inlet; b – water; c – test solution; d – test solution; f – vessel; g – solid walls. White arrows indicate observed directions.

Different from the static state, when the test solution flows through the magnetic channel, the channel changes the cross-sectional shape from round to rectangular, which has a small height and exactly the same width as the imbedded metal track. The height can be regulated by the vertical magnetic field gradient, i.e., by changing the vertical position of the chip in the bore space. To observe the frictionless flow in a magnetic channel, and to compare it with usual viscous flow in a solid channel, as shown in Fig. 5, two kinds of experiments were carried out; one is the case of a magnetic channel, which is composed of an inlet of the test solution and an iron track. The test solution is injected at the inlet flows through the magnetic channel, being recovered by a reservoir at the end of the track. As shown in Fig.5A, the whole system is immersed in water. Fig. 5B represents a solid channel composed of an inlet of the test solution and a solid channel with a solid bottom and two solid walls; the top of the channel is open, and the whole system is immersed in water. In both cases, if the solution is dragged backward by the friction of the channels, the height of the flow increases. Therefore, observing the height of the test solution, we can easily discriminate whether the flow is frictionless or not. As shown in Fig. 6a, though the injection rate increases, the height of the test solution flowing in the magnetic channel was kept constant. This is

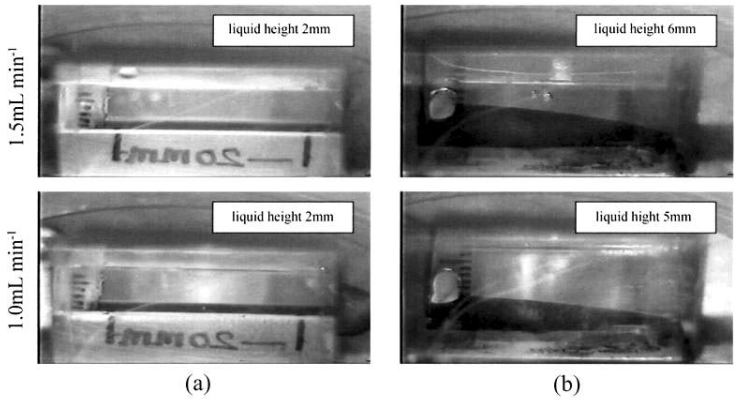

Fig. 6. Difference of flow modes in the magnetic and solid channels. Right side, the case of the magnetic channel; left side, the case of the solid channel.

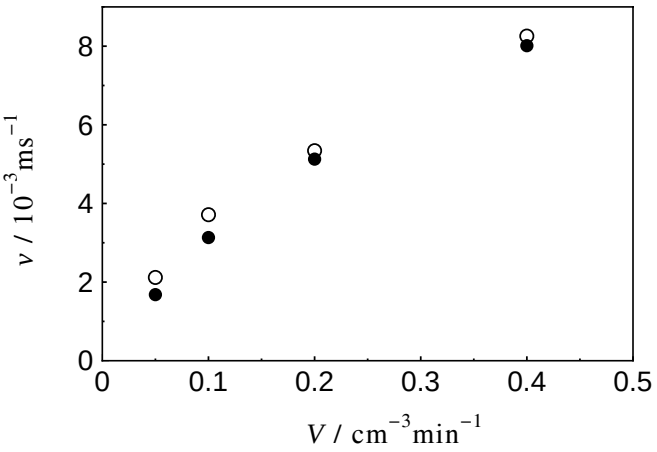

Fig. 7. Velocities of magnetic channel flow vs. injection rates. V – injection rate; v – flow velocity. Solution B (•) has a viscosity twice as high as solution A (○).

because the test solution, as mentioned above, proceeds with being sustained by the frictionless boundaries. On the contrary, in the solid channel in Fig. 6b, as the injection rate increases due to the friction of the walls, the solution height also increases. To ascertain such specific feature of the magnetic channel, with two kinds of test solutions having different viscosities, the flow velocities were measured. As shown in Fig. 7, though the kinematic viscosity of solution B (2.42 cSt) was twice as high as solution A (1.21 cSt), each velocity showed almost the same value.

Moreover, the non-viscous feature was again ensured by observing the mixing processes of the black and white test solutions in a magnetic mixing chamber and a solid mixing chamber. As shown in Fig .8a, the mixing chamber was formed by

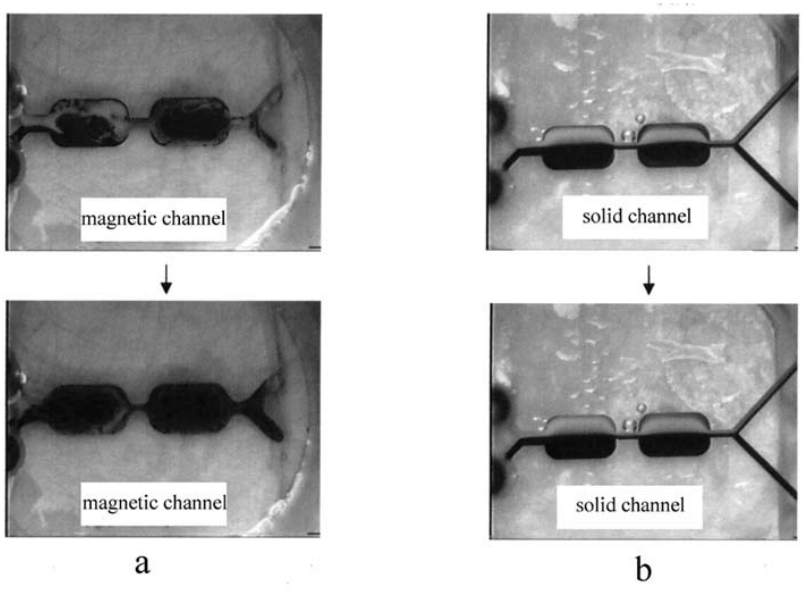

Fig. 8. Flow visualization at the mixing chambers in the magnetic and solid channels. (*a*) in the magnetic channel; (*b*) in the solid channel.

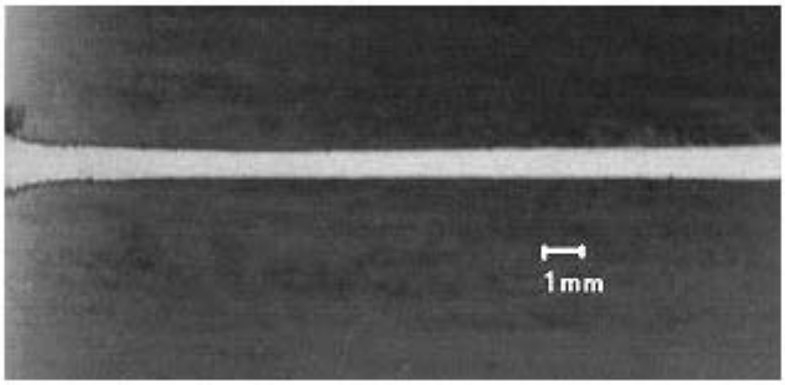

Fig. 9. Nickel deposit on a polyimide sheet by nickel electroless plating. The plating solutions were introduced in a magnetic channel formed on the sheet.

two wide portions of the magnetic channel, which are formed exactly in the same shapes as the bulges of the iron track imbedded on the chip surface. The whole chip was immersed in water. According to the frictionless boundary condition, it can be seen that in the mixing chambers, typical Kàrmàn vortex trains with approximately 100 μm in size are generated. Simultaneously, it can be also seen that white and black solutions are mixed with each other, which represents the high mixing efficiency in the magnetic mixing chambers. On the other hand, two solid mixing chambers were formed together with a solid channel, which were engraved 5 mm deep onto the chip surface. The whole chip was immersed in water. As a result, the test solutions in the solid channel were surrounded by a solid bottom and two solid walls, and the sizes of the channel (1 mm wide) and chambers (5 mm wide) were exactly the same as those in the case of the magnetic channel. As shown in Fig. 8b, due to the low Reynolds number, the black and white solutions moved in a laminar mode without mixing. After ascertaining the basic properties of the magnetic channel, by means of the magnetic channel, a new-type of electroless plating was attempted. Fig. 9 exhibits an example, i.e., nickel electroless plating on a plastic sheet. A straight path of nickel deposit was formed following an iron track (1 mm wide) placed under the plastic sheet [24].

4. Conclusion It was founded that the magnetic channel formed on the magnetic micro-fluid chip has a quite useful feature for the fluid motion, i.e., in the channel the test solution moves in frictionless mode. This is because the heterogeneous magnetic field around a ferromagnetic metal track generates a kind of channel surrounded by the magnetic walls, i.e., magnetic barriers, which keep the test solution separately from the environmental solution. Depending on the magnetism of the test solution, an environmental solution with suitable magnetism should be chosen, since the magnetic force to keep the test solution is generated not only by the magnetic field gradient, but also by the relative magnetic susceptibility determined by the difference of the magnetisms of the test and environmental solutions. The channel is surrounded not by solid, but by solution divided by the magnetic walls. Therefore, the test solution is maintained without mixing with the environmental solution, and moves in a non-viscous mode. Since the mass and heat transfers across the magnetic wall are possible, quite new types of chemical and electrochemical reactors can be made. with the magnetic channels.

REFERENCES

1. S. Mohanta, T.Z. Fahidy. *J. Appl. Electrochem.*, vol. 6 (1976), pp. 211–220.
2. T.Z. Fahidy. The effect of magnetic fields on electrochemical processes. *Modern Aspects of Electrochemistry No. 32*, pp. 333–354 (eds. R.E. White, J. O'M. Bockris, B. E. Conway, Kulwer/Plenum, New York, 1999).
3. A. Olivier, J.P. Chopart, J. Douglade, G. Gabrielli. *J. Electroanal. Chem.*, vol. 217 (1986), pp. 443–452.
4. R. Aogaki, K. Fueki, T. Mukaibo. *Denki Kagaku (Presently Electrochemistry)*, vol. 43 (1975), pp. 504–508.
5. R. Aogaki, K. Fueki, T. Mukaibo. *Denki Kagaku (Presently Electrochemistry)*, vol. 43 (1975), pp. 509–514.
6. R. Aogaki, K. Fueki. *J. Electrochem. Soc.*, vol. 131 (1984), pp. 1295–1300.
7. R. Aogaki. In*Proc. Symp. on New Magneto-Science 2000* (Omiya, Japan, 2000), pp.27–46.
8. R. Morimoto, A. Sugiyama, R. Aogaki. *Electrochemistry*, vol. 72 (2004), pp. 421–423.
9. R. Aogaki. *Magnetohydrodynamics*, vol. 39 (2003), pp. 453–460.
10. M. Asanuma, R. Aogaki. The Effect of Magnetic Fields on Electrochemical Processes. *Electrochemical Approach to Selected Corrosion and Corrosion Control Studies*, pp. 310–331. (eds. P.L. Bonora *et al.* , IOM Communications, London, 2000).
11. R. Aogaki. *Magnetohydrodynamics*, vol. 37(1-2) (2003), pp. 143–150.
12. R.N. O'Brien, K.S.V. Santhanam. *J. Appl. Electrochem.*, vol. 27 (1997), p. 573–578.
13. M. Waskaas, Y.I. Kharkats. *J. Electroanal. Chem.*, vol. 502 (2001), pp. 51-57.
14. S. Kishioka, A. Yamada, R. Aogaki, T. Kiyoshi, A. Goto, T. Shimizu. *Chem. Lett.*, (2000), pp. 656-657.
15. O. Devos, R. Aogaki. *Chem. Lett.*, (1999), pp. 169–170.
16. O. Devos, R. Aogaki. *Anal. Chem.*, vol. 72 (2000), pp. 2835–2840.
17. S. Kishioka, R. Aogaki. *Chem. Lett.*, (1999), pp. 91–92.
18. S. Kishioka, A. Yamada, R. Aogaki. *Phys. Chem. Chem. Phys.*, vol. 2 (2000), pp. 4179–4183.
19. A. Sugiyama, S. Morisaki, R. Aogaki. *Materials Transactions, JIM.*, vol. 41 (2000), pp. 1019–1025.
20. A. Sugiyama, S. Morisaki, R. Aogaki. *Jpn. J. Appl. Phys.*, vol. 42 (2003), pp. 5322–5329.
21. A. Sugiyama, M. Hashiride, R. Morimoto, Y. Nagai, R. Aogaki. *Elecrtochim. Acta*, vol. 49 (2004), pp. 5115–5124.
22. D. Figeys, D. Pinto. *Anal. Chem.*, vol. 72 (2000), pp. 330A–335A.
23. R. Aogaki, E. Ito, M. Ogata. In *Proc. Symp. on New Magneto-Science 2003*, (Tsukuba, Japan, 2003), pp.70–76.
24. M. Hashiride, R. Morimoto, M. Saito, A. Sugiyama, R. Aogaki. *Saitama Industrial Technology Center Annual Report*, vol. 2 (2004), pp. 133–136.